[11] G. L. Matthaei, D. Y. Wong, and B. P. O'Shaughnessy, "Simplifications for the analysis of interdigital surface-wave devices," *IEEE Trans. Sonics Ultrason.*, vol. SU-22, pp. 105–114, Mar. 1975.
[12] G. L. Matthaei and D. Y. Wong, "Some techniques for interdigital acoustic-surface-wave filter synthesis," in *1973 IEEE Ultrasonics Symp. Proc.* (New York), pp. 427–432.
[13] C. S. Hartmann and B. G. Secrest, "End effects in interdigital surface wave transducers," in *1972 IEEE Ultrasonic Symp. Proc.* (New York), pp. 413–416.
[14] W. R. Smith, Jr., "Circuit model analysis for interdigital transducers with arbitrary stripe-to-gap ratios, polarity sequences, and harmonic operation," in *1974 IEEE Ultrasonic Symp. Proc.* (New York), pp. 412–417.

Symmetrical Four-Port Edge-Guided Wave Circulators

PIETRO DE SANTIS, MEMBER, IEEE, AND FIORAVANTE PUCCI

Abstract—**Four-port microwave-integrated-circuit (MIC) edge-guided wave circulators (EGC) have been designed, fabricated, and tested. A mathematical characterization of the strip conductor's shape as well as a precise mechanical control of the bias inhomogeneity are provided. By means of these two techniques the reproducibility of the device is greatly improved with respect to that of the EGC obtained by the traditional cut-and-try methods.**

X-band performance data are presented and related to the spatial distribution of the effective magnetic permeability μ_{eff} in the ferrite substrate. Experimental evidence is reported that an efficient circulator action occurs when $\mu_{eff} < 0$ at some point under the central circular shield.

The spatial distribution of the RF electric field at the circulator's surface is investigated by a mechanical probing technique. It is found that in the lower part of the operation band, RF fields of considerable amplitude extend in the air in the region between the guiding edge and the substrate's edge.

I. INTRODUCTION

THE rigorous solution of a symmetrical four-port circulator by using the Green's function method [1] requires three circulation conditions to be simultaneously satisfied [2]. Each condition may be formulated in terms of an infinite series of modes and subsequently approximated by a summation over a finite number of terms.

In [2] it is demonstrated that even if a large number of modes are considered, only a few discrete frequencies exist at which perfect circulation is achieved. This result is at variance with that of a three-port circulator for which perfect circulation conditions may be met over a large frequency band [3]. Alternatively, it can be stated that a four-port junction circulator is inherently narrow band and no "continuous tracking principle" [3] can be found for it.

In light of these considerations, a study of the broadband performance of a four-port edge-guided wave circulator (EGC) [4] seems to be of particular interest. Furthermore, since no difference exists in the basic principles of operation of three-port and four-port EGC's, the experience on the former [5] could be usefully extended to the latter.

Another motivation of the present work is the fact that the results published so far on the subject [4] report on EGC's with a rather poor performance over a limited bandwidth.

In the following section a brief presentation is made of the physical principles which underlie the performance of EGC's. Subsequently, these results are applied to the design of four-port circulators. In Section IV an experimental investigation is presented on the nature of the volume-wave modes which resonate under conditions of positive effective magnetic permeability. In Section V the performance data of various types of four-port symmetrical EGC's are displayed and compared to the theoretical predictions. The paper is concluded by a study on the spatial distribution of the RF fields existing in a four-port EGC.

II. PRELIMINARY CONSIDERATIONS

In a previous work [5] the present authors reported on the construction of a three-port EGC. On that occasion a precise definition of EGC's was given in order to understand clearly how they differ from the traditional Y junction microwave-integrated-circuit (MIC) circulators.

Referring the reader to [5] for the details, here we simply recall that the distinguishing feature of an EGC is the presence of a transversal field displacement effect in the tapered sections of the device. This phenomenon is absent in a traditional MIC circulator because the impedance transformers are deposited on an isotropic substrate and is present here because the whole substrate is made of a ferrite magnetized perpendicular to the ground plane.

Manuscript received January 30, 1975; revised June 23, 1975.
The authors are with the Department of Research, Selenia S.p.A., Rome, Italy.

In this work all the four-port EGC have a coupling angle of $\pi/4$ (Fig. 1) and their strip conductor is a simply connected structure, i.e., it does not contain any "hole" [6], [7] (Fig. 2). Under these circumstances all guiding edges are curved and have a "concave" profile.

Because of the star-shaped geometry of the strip conductor, no simple modal analysis has yet appeared in the literature. In the absence of a rigorous analysis, the design of EGC's has been based, so far, on the physical principles which underlie the edge-guided wave (EGW) propagation in a semi-infinite microstrip structure. A peculiar feature of the EGW propagation is that it becomes leaky whenever the radius of curvature R of the guiding edge is finite ($R < \infty$) and the effective magnetic permeability of the ferrite is positive ($\mu_{eff} > 0$) [8]. If one transfers these results from the idealized situation of a semi-infinite geometry to the actual case of a device with a strip conductor of finite size, one may recognize that the leaky EGW's become volume-wave modes of the structure under consideration [5]. It then turns out that in any practical EGW device with curved guiding edges, unwanted volume-wave-mode resonances are present whenever $\mu_{eff} > 0$ unless suitable steps are taken to kill

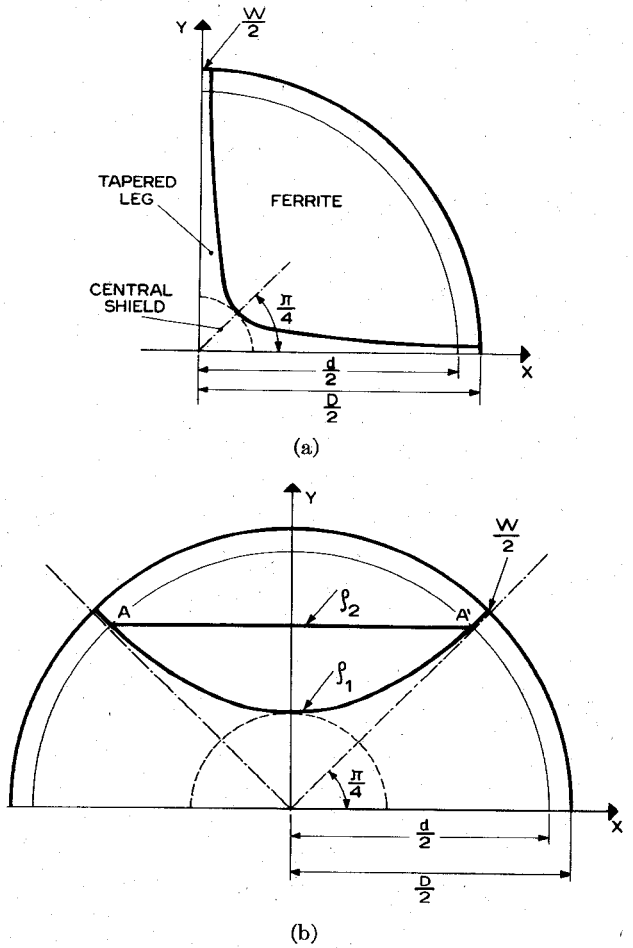

Fig. 1. (a) Coordinate axes and guiding edge profile in the hyperbolic circulator. $d = D - 2$ (millimeters). (b) Coordinate axes and guiding edge profile in the parabolic circulator. ρ_1 and ρ_2 are the limit values of the radius of the central shield (delimited by the dotted line).

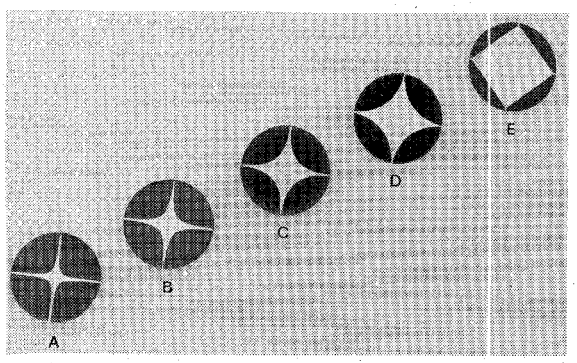

Fig. 2. Photo of some four-port EGC. From left to right: A, hyperbolic; B, cut and try; C, parabolic with $\rho = 5.23$ mm; D, parabolic with $\rho = 6.5$ mm; E, rectilinear.

them. These volume-wave resonances may be regarded as the geometrical quantization of the radiation field associated with the leaky EGW, due to the finite size of the "resonator" contained between the strip conductor and the ground plane.

We proposed a means of suppressing the spurious resonances in a three-port EGC by using an inhomogeneous magnetic bias [5]. Such a bias guarantees that $\mu_{eff} < 0$ in the central region of the circulator at those frequencies where volume-wave resonances occur. In this respect, this mode suppression technique differs from other techniques [9] based on the dissipation of the energy associated with the unwanted resonating modes. In the following sections we shall illustrate how an inhomogeneous magnetic bias also can be usefully exploited in the construction of symmetrical four-port EGC's.

III. THE DESIGN OF A FOUR-PORT EGC

The design concepts of a four-port EGC are the same as those of a three-port EGC. They can be summarized by saying that a tradeoff is to be found in order to meet simultaneously the following conflicting conditions: gradual taper sections, short guiding edges, large shield diameter, and small substrate diameter. The importance of a gradual taper has been experimentally checked by a number of authors [4], [10]. It guarantees a smooth transition between a microstrip quasi-TEM mode and an EGW mode.

In practice such a condition can be satisfied only on an empirical basis since no theory exists as yet which predicts the electromagnetic (EM) field in the tapered sections of an EGW device [11], [12]. Note that a slow tapering rate requires a minimum length of the tapered sections below which the excitation of the EGW becomes very poor. Also, as a consequence, the circulator's substrate has a minimum diameter below which no efficient circulation is observed.

The advantage of short guiding edges is due to the fact that the attenuation of an EGW is proportional to the length of the guiding edge. If the guiding edge is rectilinear, dielectric and magnetic losses in the substrate as well as ohmic losses in the metal conductors are largely responsible for the attenuation. They have been calculated

[11]–[13] by formally introducing into the results of the lossless analysis complex values for the constitutive parameters of the ferrite material and a finite value for the conductivity of the metal conductors. Typically [11], for a semi-infinite microstrip on a ferrite substrate (relative dielectric constant $\epsilon_f = 14.5$, dielectric tan $\delta = 2 \times 10^{-4}$, saturation magnetization $4\pi M_S = 1$ kOe, $\Delta H_{\text{eff}} = 5$ Oe, thickness $h = 2$ mm, applied magnetic bias $H_0 = 1.3$ kOe) an attenuation of 0.03 dB/cm was calculated for frequencies between 4 and 10 GHz. If the guiding edge is concave and μ_{eff} is positive, mode conversion into volume-wave modes is an additional source of loss. However, no quantitative evaluation of this type of loss has yet appeared in the literature. Only the radiation loss of an EGW propagation along the concave edge of a semi-infinite microstrip circuit was calculated [8]. Typically, an attenuation of 0.04 dB/cm was found at 10 GHz in YIG microstrip with a radius of curvature of 8 cm. The condition requiring a large shield diameter guarantees that the EGW has a transversal decay under the metallization sufficiently rapid to avoid the excitation of other edges. Although the validity of such a condition can be easily ascertained by extending to the circulator the results found for the isolator [10], an exact evaluation of the transversal decay rate of an EGW in a circulator requires the solution of the boundary value problem relative to the structure under consideration. Since no such solution as yet exists, the diameter of the central shield also is chosen, in general, on an empirical basis.

The last condition requires a small substrate diameter. This condition is directly related to the size and weight of the device. In an EGC the whole substrate is, in fact, magnetized and the permanent magnet's diameter is at least equal to that of the substrate.

In addition to these geometrical conditions, the ferrite material must have suitable physical properties. In particular the linewidth ΔH must be small and the saturation magnetization $4\pi M_S$ must be large.

The importance of having a small ΔH is obvious. The usefulness of a large $4\pi M_S$ has been pointed out in [10] and [14] in connection with EGW isolators, and is expected to be valid also in the present case. For X-band performance it was decided that a YIG material with $4\pi M_S = 1780$ Oe and a relative dielectric constant $\epsilon_f = 14$ was a suitable one.

As far as the shape of the strip conductor was concerned, our choice was in favor of guiding edges with a spatially variable radius of curvature. Circulators with both hyperbolic and parabolic profiles were constructed and tested. The choice of these particular types of profile was dictated by the fact that they were amenable to an exact mathematical characterization. The ratio W/h of the strip conductor's width at the four ports to the substrate's thickness was chosen as if the ferrite were a dielectric with $\epsilon_f = 14$ and $\mu_{\text{eff}} = 1$ [15]. Although this is not always true in our circulators because within the operation band μ_{eff} changes from ~ 1 to large negative values, previous experience on three-port EGC's has shown that this choice is a good one. The diameter D of the substrate was chosen to be 30 mm. This value was found to be the minimum value which would guarantee a good performance of the circulator. It was slightly larger than that of a three-port EGC which was 22 mm. The height of the ferrite substrate was, in general, chosen to have the standard value of 0.6 mm although a circulator with $h = 0.95$ mm was also fabricated. Once the three quantities W, h, and D are fixed, and each circulator's arm begins with a rectilinear segment of length 1 mm to guarantee good contacts, the hyperbolic profile is uniquely defined by the equation [Fig. 1(a)]

$$y = \frac{Wd}{4x} \tag{1}$$

where $d/2 = D/2 - 1$ mm. The parabolic profile, on the other hand, may be chosen, within the set of curves [Fig. 1(b)]

$$y = \frac{2(2)^{1/2}(d + W) - 8\rho}{(d - W)^2} x^2 + \rho \tag{2}$$

where ρ is a parameter representing the radius of the central shield of the circulator (dotted line in Fig. 1) which may vary between the limit values

$$\rho_1 = \frac{1}{4(2)^{1/2}} (d + 3W)$$

and

$$\rho_2 = \frac{(2)^{1/2}}{4} (d + W).$$

These two values, respectively, define a circulator with $|dy/dx| = 1$ at the points A and A', of Fig. 1(b) and a "square" circulator.

Fig. 2 is a photograph of some circulators which have been constructed by usual MIC photolithographic techniques. The strip conductor's profile is: A, hyperbolic; B, obtained by cut-and-try to lie between cases A and C without any mathematical characterization; C, parabolic with $\rho = 5.23$ mm; D, parabolic with $\rho = 6.5$ mm; E, rectilinear. The substrate thickness is $h = 0.64$ mm in all cases.

IV. THE HOMOGENEOUS MAGNETIC BIAS

In order to observe the spurious volume-wave resonances in a four-port EGC, the structures of Fig. 2 were immersed in a homogeneous magnetic bias $H_0 = 3150$ Oe, applied perpendicular to the ground plane, i.e., along the coordinate Z axis. Under these circumstances the insertion loss between two adjacent ports (the remaining two being matched to a 50-Ω load) behaves as shown in Fig. 3. Here the zero-dB insertion loss points are represented by the thin solid line. A vertical dashed line is also drawn at $\mu_{\text{eff}} = 0$ to highlight the fact that spikes exist only when $\mu_{\text{eff}} > 0$. The numbers between parentheses indicate the area in square millimeters of the central shield of the circulators. Fig. 3 clearly shows that as the "resonator's" volume is increased by increasing the area of the strip

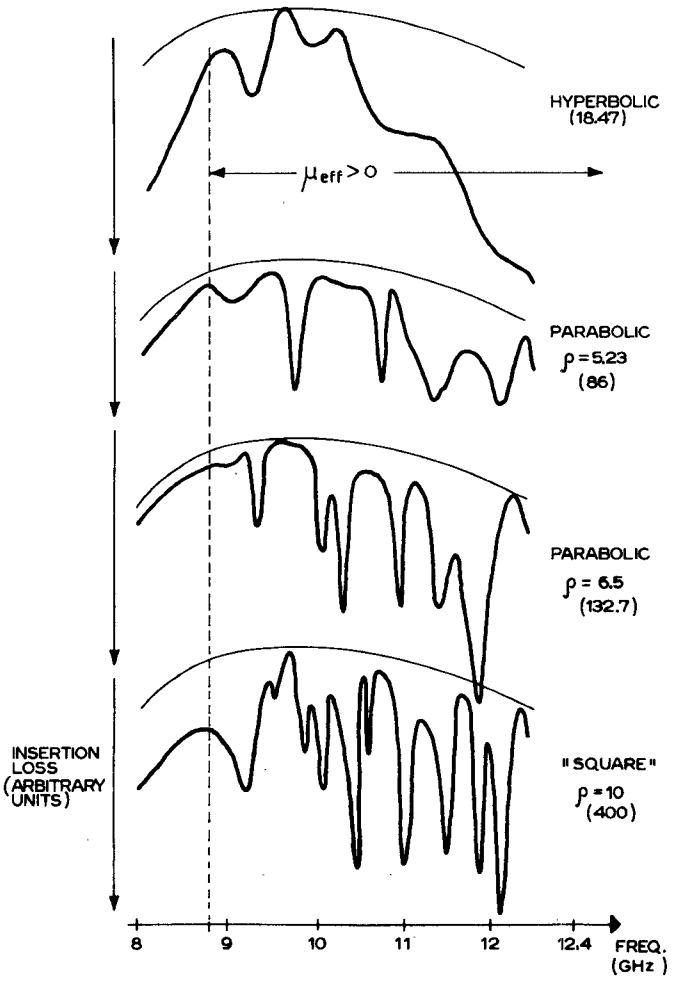

Fig. 3. Insertion loss versus frequency diagrams for the structures A,C,D,E of Fig. 2 immersed in a dc magnetic field of 3150 Oe.

conductor, the number of resonances in the frequency range 9–12 GHz also increases. No such phenomenon occurs if the resonator's volume is changed just by increasing the substrate's thickness and keeping the area of the central shield unaltered. This confirms the known result that all the observed spikes are Z-independent volume-wave resonances whose frequencies are determined by the geometrical dimensions of the central shield. As previously anticipated, the observed resonances can be suppressed by using a suitable inhomogeneous magnetic bias. Fig. 4 shows three among various magnetic bias profiles which were tried in our circulators. Here r indicates the distance in millimeters from the axis of the circulator. Since H_0 enjoys a rotational symmetry, it is measured by just displacing a Hall probe in a radial direction slightly above the RF conductor. During the feasibility studies of the device, the inhomogeneous magnetic bias was generated by suitably shaping the pole pieces of the electromagnet [Fig. 5(a)].

Values of a,b,c corresponding to the various bias profiles are shown in Fig. 4. In the final version of the device the inhomogeneous magnetic bias has been obtained by suitably shaping the ground plane as shown in Fig. 5(b). Here ① is two permanent magnets, ② is a soft-iron support, ③ is an annulus of brass, ④ is the ferrite microstrip circuit, and ⑤ is a layer of low dielectric constant. A control of the bias profile was achieved by varying the diameter of the small soft-iron cylinder. In the following section it will be shown that a proper choice of the bias profile allows the construction of a broad-band four-port ECC circulator.

V. EXPERIMENTAL RESULTS

In this section the performance data are presented of the structures shown in Fig. 2 immersed in an inhomogeneous magnetic bias of the type shown in Fig. 4. All the circulators under test have $h = 0.64$ mm, $W = 0.42$ mm, $D = 30$ mm, and are connected to the external circuit by means of coaxial-to-microstrip Tek Wave transitions APC 7.

The measurements are at X band and include the insertion loss between two adjacent ports, the isolation between uncoupled ports, and the VSWR at each port. The measured values are considered to be "good" if they are, respectively, smaller than 1 dB, higher than 20 dB, and smaller than 1.25.

The hyperbolic circulator displayed a good performance only over a limited bandwidth of the order of 1 GHz. This result was obtained by using the magnetic bias Ⓐ of Fig. 4. Every attempt to broad-band the device by

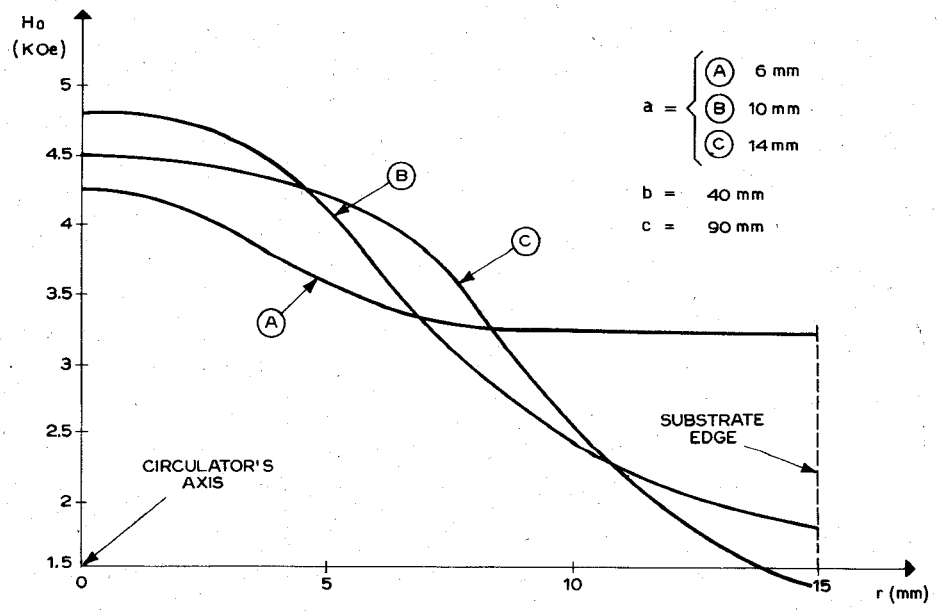

Fig. 4. Typical magnetic bias profiles used for the circulators of Fig. 2. The dimensions a, b, c are defined in Fig. 5(a).

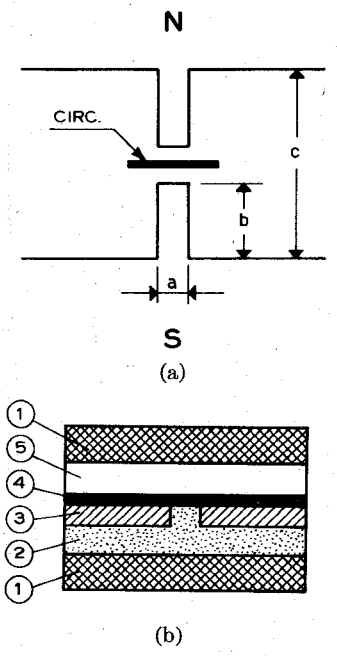

Fig. 5. Pole pieces used to shape the applied dc magnetic field. (a) Electromagnet. (b) Permanent magnet.

means of a different magnetic bias caused a higher insertion loss.

The cut-and-try circulator has a slightly larger operational bandwidth. The parabolic circulator with $\rho = 5.23$ presents a fairly good performance over the whole X band when H_0 has the profile Ⓑ of Fig. 4. Its performance has the following typical values: insertion loss, 1 dB; isolation (adjacent ports), 30 dB; isolation (opposite ports), 20 dB; VSWR $\simeq 1.25$.

The parabolic circulator with $\rho = 6.5$ immersed in the magnetic bias Ⓒ of Fig. 4 yielded the best results and its performance data are shown in Figs. 6 and 7. Every attempt to eliminate the volume-wave resonances in the "square" circulator was unsuccessful.

In Figs. 6 and 7 the dashed thin curves are calibration curves. In the isolation versus frequency diagram of Fig. 6, the continuous heavy curve is relative to opposite ports whereas the heavy dashed curve is relative to adjacent ports.

In the diagram of Fig. 7 the four curves represent the input VSWR at the four ports of the circulator. The results display a good fourfold symmetry. A comparison between the insertion loss curve and the corresponding curve in Fig. 3 reveals how the chosen inhomogeneous magnetic bias efficiently kills all the spurious resonances. The fact that the insertion loss is always below 1 dB, the connectors' loss being included, validates *a posteriori* the criterion presented in Section III of choosing W/h ac-

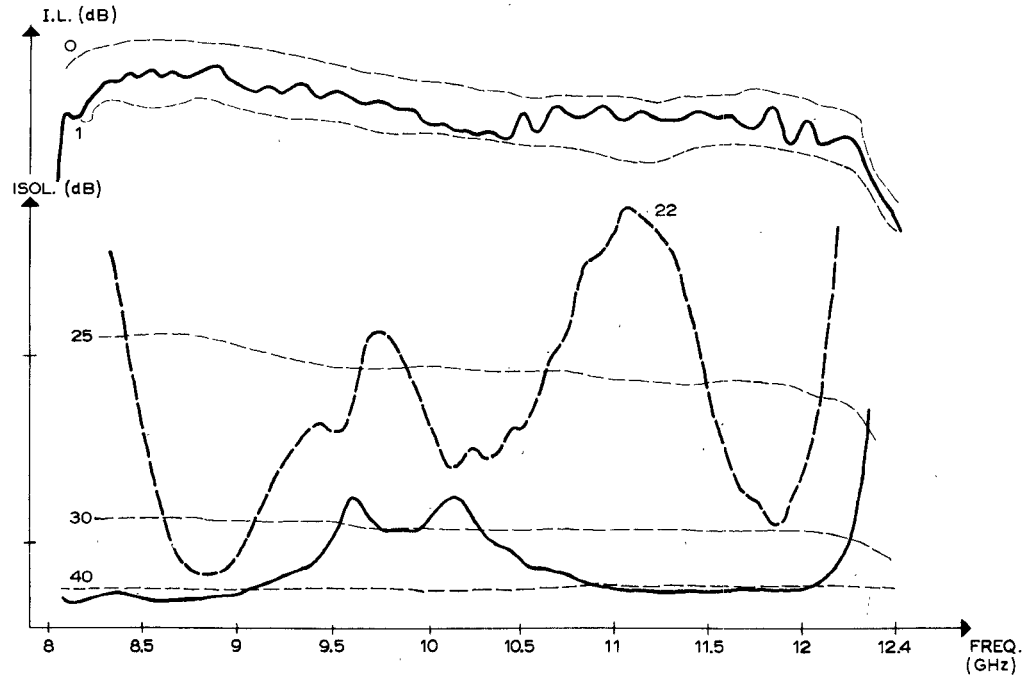

Fig. 6. Performance data of the parabolic circulator with $\rho = 6.5$ mm immersed in the magnetic bias © of Fig. 4. The isolation curves refer to opposite ports (dashed) and adjacent ports (continuous).

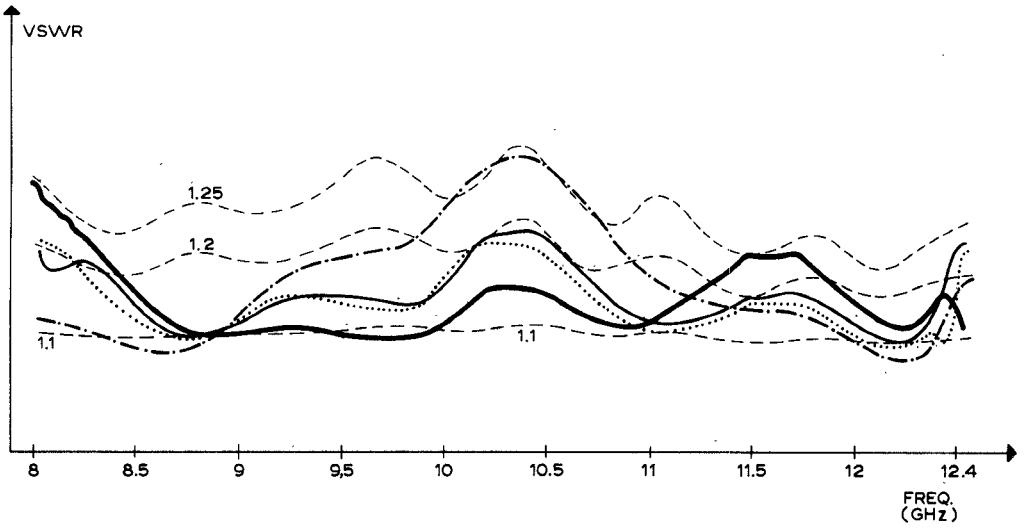

Fig. 7. VSWR at the four ports of the circulator of Fig. 6.

cording to Schneider's curves [15]. In order to gain a deeper physical insight into the performance of a circulator with an inhomogeneous magnetic bias, the spatial inhomogeneity of H_0 was related to the spatial behavior of the effective magnetic permeability μ_{eff} of the ferrite's substrate. For the parabolic circulator with $\rho = 6.5$ this was done graphically by means of the composite diagram of Fig. 8. The diagram is subdivided into three parts labeled with roman numerals. Part I represents half of the circulator. The drawing's scale is 1: 0.375. In part II the experimental values of $H_0(r)$ which gave the best circulator performance are reported. Part III is the first quadrant of the H_0 versus f coordinate plane, f being the operation frequency. The two oblique heavy lines represent the locii where $\mu_{\text{eff}} = 0, \infty$. For completeness we recall that they are defined by the equations

$$H_0 = f/\gamma - 4\pi M_S + H_d \tag{3}$$

$$f/\gamma = [(H_0 - H_d)^2 + (H_0 - H_d)4\pi M_S]^{1/2} \tag{4}$$

where $H_d = 4\pi M_S = 1780$ Oe is the dc demagnetizing field and γ is the gyromagnetic ratio. These two lines partition the coordinate plane into three zones wherein μ_{eff} may be either positive or negative. More specifically, $\mu_{\text{eff}} < 0$ between the two lines and $\mu_{\text{eff}} > 0$ elsewhere.

From this diagram one determines the algebraic sign of μ_{eff} at a given frequency in a given point of the circulator. For example, if one wants to know the algebraic sign of

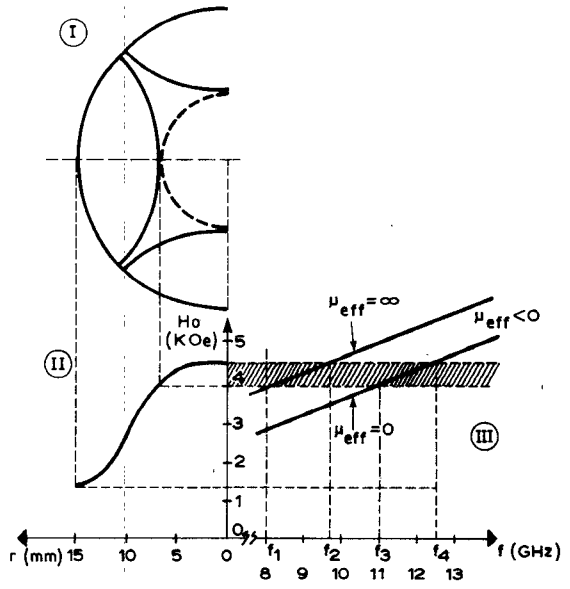

Fig. 8. Diagram used to find the algebraic sign of μ_{eff} at various points of the parabolic circulator with $\rho = 6.5$ mm. $H_0(r)$ is the bias profile which gives the best results.

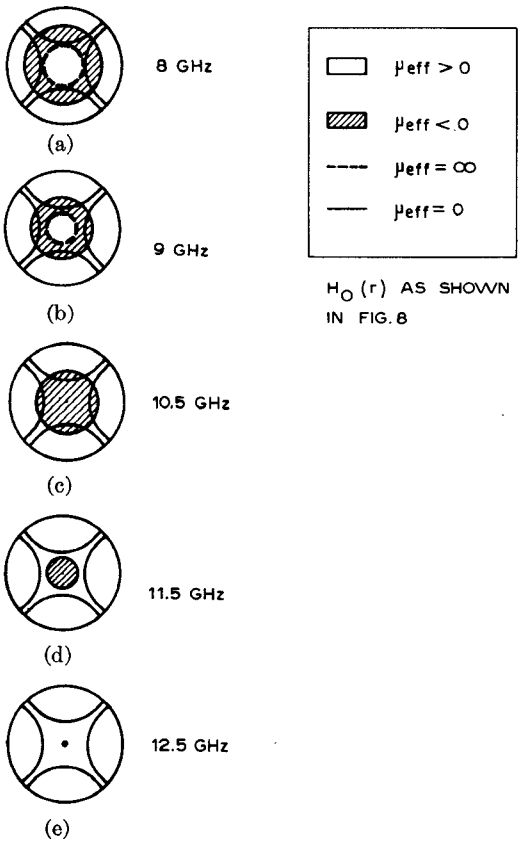

Fig. 9. Spatial distribution of μ_{eff} as derived from Fig. 8.

μ_{eff} for the points under the central shield one must refer to the shaded area in part III. Fig. 9 shows the spatial distribution of μ_{eff} as derived from Fig. 8.

At the limit frequency $f_1 = 8$ GHz, $\mu_{eff} = \infty$ along the circumference indicated by a dashed line in Fig. 9(a). This means that heavy magnetic losses are present in the central region of the guiding edges, and consequently the device displays a large insertion loss (see Fig. 6).

As the operation frequency increases from f_1 to f_2, the lossy region associated to the $\mu_{eff} = \infty$ condition moves toward the center of the central shield [Fig. 9(b)]. In this frequency range, however, the measured insertion loss is small, indicating that the EGW transversal decay under the metallization is so rapid that most of the RF power flows outside the lossy region. In the following section we shall report experimental data showing that at these frequencies a considerable amount of RF power exists in the air just above the unmetallized part of the substrate. All these observations tend to demonstrate that in this frequency range most of the RF power flows outside the central shield. Whether this is still an EGW mode remains to be established and the reader is referred to the next section for a further discussion on this point. For frequencies between f_2 and f_3, $\mu_{eff} < 0$ at all points under the central shield. The situation is depicted in Fig. 9(c). For frequencies between f_3 and f_4 the ferrite material has $\mu_{eff} < 0$ in a disk-shaped region under the central part of the shield [Fig. 9(d)]. As frequency increases such a region shrinks, and eventually disappears at $f = f_4$. At the upper limit frequency $f_4 = 12.5$ GHz all the ferrite under the shield has $\mu_{eff} > 0$ and efficient circulation ceases to exist (see Figs. 6 and 7). For operation frequencies higher than 12.5 GHz, in fact, the whole substrate has a positive μ_{eff} and resonating volume-wave modes start being observed. From what follows one can recognize that the bias profile $H_0(r)$ which gives the best results is the one which guarantees $\mu_{eff} < 0$ at some point under the central shield, i.e., in that region where volume-wave modes may resonate.

VI. THE RF FIELD DISTRIBUTION

In the previous section it was shown that at a given frequency μ_{eff} may be either positive or negative in different regions of the ferrite's substrate. In a cylindrical geometry this is equivalent to saying that the spatial distribution of the RF fields may be either oscillatory or decaying in different regions of the ferrite's volume. Unfortunately, no mechanical probing of the RF fields can be made within the ferrite volume. One can only probe the RF fields in the air just above the substrates's surface. Previous authors [16], [17] have used this type of probing, in connection with Y- junction MIC circulators, and found that a new mode, the "wall-affected" mode, is responsible for the broad-band operation of the device. We have carried out a similar type of probing in our four-port EGC's. Fig. 10 displays a set of recorded patterns as obtained by a vertical electric probe displaced parallel to and just above the circulator's substrate. In Fig. 10 the scanning line is radial, midway between two adjacent ports (dashed line in the insert of Fig. 10). From this diagram and from the RF field profiles probed in various regions of the circulator surface, the conclusion is reached that the amplitude of the RF fields between the substrate's and strip conductor's edges in the frequency range 8–9.5 GHz is much larger than for frequencies higher than 9.5.

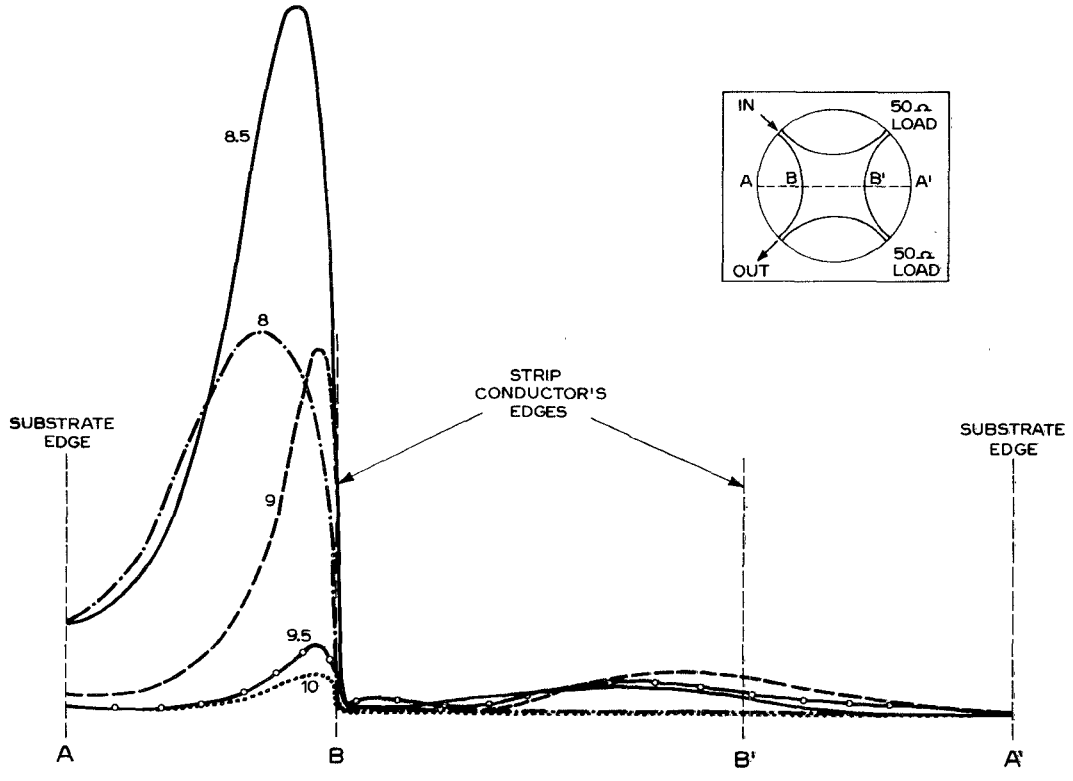

Fig. 10. Probed RF electric field at the circulator's surface. The dotted line in the insert is the scanning line. The numbers indicate the frequency in gigahertz.

Furthermore, from Fig. 10 one can appreciate how between 8 and 9.5 GHz the electric field at the substrate's edge is still of appreciable magnitude. This behavior is very similar to that observed by Miura and Hashimoto [16], [17] and seems to be present in MIC circulators with an all-ferrite substrate. The exact nature of the wall-affected mode and how it relates to the edge-guided modes remains to be established and deserves further attention.

VII. CONCLUSIONS

It has been demonstrated that by use of a suitable magnetic bias the broad-band performance characteristics of a three-port EGC can be extended to a four-port EGC.

In this paper a number of improvements have been introduced in the study and construction of an EGW device. In particular, a mathematical characterization of the strip conductor's shape as well as a precise mechanical control of the magnetic bias profile have been achieved.

With reference to a ferrite substrate of diameter D = 30 mm and thickness h = 0.64 mm it has been shown that the best X-band performance is obtained by means of parabolic strip conductor profiles with ρ = 6.5 mm and magnetic bias profiles with $H_{0,\max}$ = 4500 Oe and $H_{0,\min}$ = 1440 Oe. A deeper physical insight into the mechanism which allows a correct circulator action over a large bandwidth has been gained by finding the spatial distribution of $\mu_{\text{eff}}(r)$ in correspondence to $H_0(r)$. It has been shown that unwanted volume-wave resonances are efficiently killed whenever $\mu_{\text{eff}} < 0$ at some point under the central shield. This result evidences the substantial difference between this mode-suppressing technique and the stagger-tuning phenomena present in MIC circulators biased by an inhomogeneous dc magnetic field [18].

As compared to the three-port EGC, the constructed four-port circulator presents both a larger diameter and a higher bias. However, no optimization studies have been undertaken concerning these two quantities.

Although the preceding experimental results demonstrate that a good MIC four-port EGC is feasible at X band the theory of this device seems to be at a rather early stage. In particular, a modal analysis of a star-shaped MIC circuit is still lacking and no exact knowledge exists on EGW propagation in transversally inhomogeneous transmission lines.

Finally, we believe that additional attention should be given to the problem of finding a relation between the wall-affected mode and the EGW mode.

ACKNOWLEDGMENT

The authors wish to thank Dr. C. Mistano and E. Simonetti for the construction of the circulators.

REFERENCES

[1] H. Bosma, "On stripline Y-circulation at UHF," *IEEE Trans. Microwave Theory Tech. (1963 Symp. Issue)*, vol. MTT-12, pp. 61–72, Jan. 1964.
[2] W. H. Ku and Y. S. Wu, "On stripline four port circulator," in *1973 IEEE G-MTT Int. Microwave Symp. Dig.* (Boulder, CO), pp. 86–88.
[3] Y. S. Wu and F. J. Rosenbaum, "Wideband operation of microstrip circulators," in *1973 IEEE G-MTT Int. Microwave Symp. Dig.* (Boulder, CO), pp. 92–94.

[4] M. E. Hines, "Ferrite transmission devices using the edge-guided mode propagation," in *1972 IEEE G-MTT Int. Microwave Symp. Dig.* (Chicago, IL), pp. 236–237.
[5] P. de Santis and F. Pucci, "The edge-guided-wave circulator," *IEEE Trans. Microwave Theory Tech.*, vol. MTT-23, pp. 516–519, June 1975.
[6] ——, "Novel type of MIC symmetrical three-port circulator," *Electron. Lett.*, vol. 8, pp. 12–13, Jan. 1972.
[7] ——, "Experiments on the optimization of a novel MIC symmetrical three-port circulator," in *1972 IEEE G-MTT Int. Microwave Symp. Dig.* (Chicago, IL), pp. 238–240.
[8] P. de Santis, "Edge guided modes in ferrite microstrips with curved edges," *Appl. Phys.*, vol. 4, pp. 167–174, Aug. 1974.
[9] R. Anderson, U. S. Patent 3 555 459, Jan. 12, 1971.
[10] L. Courtois, B. Chiron, and G. Forterre, "Propagation dans une lame de ferrite aimantée. Application à de noveaux dispositifs non réciproques a large bande," *Cables Transmission*, pp. 416–435, Oct. 1973.
[11] L. Courtois, G. Forterre, and B. Chiron, "Improvement in broadband ferrite isolators," presented at the 20th Annu. Conf. Magnetism and Magnetic Materials (San Francisco, CA, Dec. 1974), Paper 2E-11.
[12] ——, "A survey of broadband stripline ferrite isolators," in *1975 Intermag. Conf. Dig.* (London), pp. 7–9.
[13] P. de Santis and G. Cortucci, "Edge-guided waves in lossy ferrite microstrips," in *1973 Proc. European Microwave Conf.* (Brussels, Sept. 4, 1973), vol. 3, p. B.9-1.
[14] M. Blanc, L. Dusson, and J. Guidevaux, "Etudes de dispositifs non réciproques a ferrite à très large bande. Premières realizations," Thomson-CSF Tech. Rep., vol. 4, pp. 27–48, Mar. 1972.
[15] M. U. Schneider, "Microstrip lines for microwave integrated circuits," *Bell Syst. Tech. J.*, vol. 48, pp. 1421–1444, May–June 1969.
[16] T. Miura and T. Hashimoto, "A new concept for broadbanding the ferrite substrate circulator based on experimental modal analysis," in *1971 IEEE G-MTT Int. Microwave Symp. Dig.*, pp. 80–81.
[17] S. March, "Comments on 'A new concept for broadbanding the ferrite substrate circulator based on experimental modal analysis,'" *IEEE Trans. Microwave Theory Tech.*, vol. MTT-22, pp. 71–74, Jan. 1974.
[18] B. Hershenov, "Microstrip junction circulator for microwave integrated circuits," *IEEE Trans. Microwave Theory Tech.* (Corresp.), vol. MTT-15, pp. 748–750, Dec. 1967.

Rate Effects in Isolated Turtle Hearts Induced by Microwave Irradiation

CHARLES E. TINNEY, JAMES L. LORDS, AND CARL H. DURNEY, MEMBER, IEEE

Abstract—**Microwave irradiation at 960-MHz CW of isolated poikilothermic hearts in Ringer's solution causes bradycardia. Tachycardia is usually produced by generalized heating, suggesting the possibility of a different mechanism in this case. The effect occurs only over a narrow power range of approximately 2–10 mW/g absorbed by the heart. It is hypothesized that microwave radiation causes neurotransmitter release either by excitation of the nerve remnants in the heart, or by some other mechanism, producing bradycardia over a restricted range of power absorption. Drugs which can change the response of the heart to transmitter substances have been used, and the results support a neurotransmitter release hypothesis. A generalized heating effect, causing tachycardia, is predominant at higher levels of absorbed power.**

I. INTRODUCTION

IN a previous publication [1] we presented a series of experiments which were specifically designed to help further understand microwave biological interactions. Those experiments indicated a necessity for further work to consider interactions in a power range where generalized heating of the whole organism could not have been the principal mechanism of interaction. The present paper further describes effects that cannot be explained by generalized heating and might lead to a better understanding of mechanisms of interaction between electromagnetic fields and biological systems.

Our previous work led us to hypothesize that possible neural effects could be detected in microwave experiments performed on isolated poikilothermic heart systems. In those experiments isolated turtle hearts submerged in Ringer's solution were exposed to CW, 960-MHz microwave irradiation while both heart rate and force of contraction were being measured. The stability of the preparation and the size of the turtle heart made manipulations simple and also made the detection of any small perturbations to the system appear as reliable indicators. Agar–KCl electrodes were used as mounts to avoid possible artifacts introduced by concentration of electromagnetic fields, which occur with metal electrodes [2].

We found that microwave irradiation at approximate absorbed powers of 2–10 mW/cm^3 caused bradycardia (decrease in heart rate), while generalized heating caused tachycardia (increase in heart rate). At approximate absorbed power levels of 16–40 mW/cm^3, we found that microwave irradiation produced tachycardia. Several

Manuscript received March 28, 1974; revised August 6, 1975. This work was supported by the Office of Naval Research under Contract N00014-67-A-0325-0009.

C. E. Tinney is with the Biosystems Department, Naval Undersea Center, San Diego, CA.
J. L. Lords is with the Departments of Biology and Electrical Engineering, University of Utah, Salt Lake City, UT 84112.
C. H. Durney is with the Department of Electrical Engineering, University of Utah, Salt Lake City, UT 84112.